1-14-2005

Mapping the ρ1 GABAC Receptor Agonist Binding Pocket

Anna Sedelnikova

Craig D. Smith

Stanislav O. Zakharkin

Delores Davis

David S. Weiss

See next page for additional authors

THE JOURNAL OF BIOLOGICAL CHEMISTRY
Vol. 280, No. 2, Issue of January 14, pp. 1535–1542, 2005
Printed in U.S.A.

Mapping the ρ_1 $GABA_C$ Receptor Agonist Binding Pocket

CONSTRUCTING A COMPLETE MODEL*

Received for publication, August 30, 2004, and in revised form, November 17, 2004
Published, JBC Papers in Press, November 17, 2004, DOI 10.1074/jbc.M409908200

Anna Sedelnikova‡, Craig D. Smith§, Stanislav O. Zakharkin¶, Delores Davis‡, David S. Weiss‡, and Yongchang Chang‡‖

From the ‡Departments of Neurobiology and Physiology and Biophysics, §The Center for Biophysical Sciences and Engineering, and the ¶Department of Biostatistics, University of Alabama at Birmingham, Alabama 35294

γ-Aminobutyric acid (GABA) is the major inhibitory neurotransmitter in the mammalian brain. The GABA receptor type C ($GABA_C$) is a ligand-gated ion channel with pharmacological properties distinct from the $GABA_A$ receptor. To date, only three binding domains in the recombinant ρ_1 $GABA_C$ receptor have been recognized among six potential regions. In this report, using the substituted cysteine accessibility method, we scanned three potential regions previously unexplored in the ρ_1 $GABA_C$ receptor, corresponding to the binding loops A, E, and F in the structural model for ligand-gated ion channels. The cysteine accessibility scanning and agonist/antagonist protection tests have resulted in the identification of residues in loops A and E, but not F, involved in forming the $GABA_C$ receptor agonist binding pocket. Three of these newly identified residues are in a novel region corresponding to the extended stretch of loop E. In addition, the cysteine accessibility pattern suggests that part of loop A and part of loop E have a β-strand structure, whereas loop F is a random coil. Finally, when all of the identified ligand binding residues are mapped onto a three-dimensional homology model of the amino-terminal domain of the ρ_1 $GABA_C$ receptor, they are facing toward the putative binding pocket. Combined with previous findings, a complete model of the $GABA_C$ receptor binding pocket was proposed and discussed in comparison with the $GABA_A$ receptor binding pocket.

$GABA_A$[1] and $GABA_C$ receptors are both GABA-gated chloride channels but with very different pharmacological properties. In fact, that is the basis for their classification. Although both types of receptors can be activated by GABA, the $GABA_A$ receptor can be specifically antagonized by bicuculline. In contrast, the $GABA_C$ receptor is insensitive to bicuculline but can be selectively antagonized by 1,2,5,6-tetrahydropyridine-4-yl)-methylphosphinic acid (1). The functional properties of these two types of GABA receptors are also different. For example, the $GABA_C$ receptor has higher GABA sensitivity but slower activation and deactivation kinetics than the $GABA_A$ receptor (2). The $GABA_C$ receptor also shows almost no desensitization (2), whereas the $GABA_A$ receptor exhibits strong desensitization (3). Although the functional differences could arise from differences in the structural architecture of the GABA binding pockets, distinct antagonist profiles of $GABA_A$ and $GABA_C$ receptors indicate that their agonist/antagonist binding pockets are not the same. Studies over the last 15 years have shaped a relatively complete model for the $GABA_A$ receptor (4–9). In contrast, structural information on the $GABA_C$ receptor agonist binding pocket is far from complete. Some candidate binding residues in several potential "binding loops" are still undefined.

GABA-gated ion channels belong to the ligand-gated ion channel family, which also includes nicotinic acetylcholine receptors, serotonin-3 receptors, and glycine receptors. The study of nicotinic receptors in the past two decades has shaped a structural model for the ligand-gated ion channel family. In this model, six loops designated A–F have been identified to participate in the formation of the agonist binding pocket (10). This structural model was further confirmed and extended by the crystal structure of the homologous acetylcholine-binding protein, AChBP (11). Cumulating evidence suggests a similar general structural architecture for all members of this ligand-gated ion channel family. For example, in the GABA receptor, two ligand binding domains identified in the β_2 subunit (4) and the ρ_1 subunit (2) can be mapped to the homologous residues in loops B and C. One binding domain identified in the α_1 subunit (5, 12) and also in the ρ_1 subunit (13) can be mapped to loop D in the complementary face. More recently, two residues contributed from loop A of the β_2 subunit (7), three residues from loop F (8), and two residues from loop E of the α_1 subunit of the $GABA_A$ receptor have been identified as binding residues (9). Furthermore, the secondary structure of the GABA receptor is in agreement with the AChBP-based structural model (6–8). Due to agonist specificity and sequence diversity, key residues involved in agonist binding in different ligand-gated ion channels are not the same. Nevertheless, the similarity of the general architecture in this receptor family suggests that the AChBP-based structural model can be used as a guideline in search of the complete model of the GABA receptor agonist binding pocket.

The substituted cysteine accessibility method was first implemented in ion channels to identify pore-lining residues in nicotinic and GABA receptors (14–16). This approach is based on a functional effect of modification of the substituted cysteine by a water-soluble sulfhydryl-reactive compound. If such a modification occurs in a functionally important domain of the receptor, it is likely to produce a change in receptor function.

* This research was supported by National Institutes of Health Grant NS35291 (to D. S. W.) and Training Grant DK07545 (to Y. C.). The costs of publication of this article were defrayed in part by the payment of page charges. This article must therefore be hereby marked "*advertisement*" in accordance with 18 U.S.C. Section 1734 solely to indicate this fact.

‖ To whom correspondence should be addressed: Division of Neurobiology, Barrow Neurological Institute, 350 West Thomas Rd., Phoenix, AZ 85013. Tel.: 602-406-6192; Fax: 602-406-4572; E-mail: yongchang.chang@chw.edu.

[1] The abbreviations used are: GABA, γ-aminobutyric acid; $GABA_A$, GABA receptor, type A; $GABA_C$, GABA receptor, type C; AChBP, acetylcholine-binding protein; 3-APA, 3-aminopropylphosphonic acid; MTSET, methanethiosulfonate ethyltrimethylammonium.

By testing the functional effect of a water-soluble cysteine modification reagent and blockability of this effect by agonist and antagonist, the substituted cysteine accessibility method has also been successfully used to probe the binding sites of the $GABA_A$ (6, 17) and nicotinic receptors (18, 19). With this approach, novel residues involved in agonist binding were identified, and the secondary structures of the newly identified domain were predicted (6, 7).

In this study, using cysteine accessibility scanning and agonist/antagonist protection tests, we have identified amino acid residues involved in agonist binding in novel regions of the ρ_1 $GABA_C$ receptor subunit corresponding to loops A and E in nicotinic receptor subunits. The newly identified binding residues in loop A and part of loop E are in comparable positions as in the $GABA_A$ receptor. Moreover, in the extended stretch of loop E, a region previously unexplored in GABA-gated ion channels, we have identified three novel binding residues in the ρ_1 $GABA_C$ receptor. In contrast to the $GABA_A$ receptor, loop F in the ρ_1 homomeric $GABA_C$ receptor does not appear to be involved in agonist binding. Using the AChBP crystal structure as a template, we have built a homology model for the amino-terminal domain of the ρ_1 GABA receptor. These newly discovered binding residues, along with previously identified binding residues, are mapped to the homology model to construct a complete agonist binding pocket for the $GABA_C$ receptor.

EXPERIMENTAL PROCEDURES

Mutagenesis and cRNA Preparation—The cDNA encoding the human ρ_1 GABA receptor subunit was cloned into the pGEMHE vector in the T7 orientation (20). The residues in the amino-terminal segments corresponding to loops A, E, and F in nicotinic receptor subunits were mutated to cysteine, one at a time, using the PCR-based QuikChange method of site-directed mutagenesis (Stratagene, Hercules, CA). The mutations were confirmed by automated DNA sequencing. The fragments containing individual mutations were subcloned and resequenced to avoid additional mutations. The wild type and mutant cDNAs were then linearized by NheI digestion. The cRNAs were transcribed by standard *in vitro* transcription protocols. Briefly, RNase-free DNA templates were prepared by treating linearized DNA with proteinase K. cRNAs then were transcribed by T7 RNA polymerase. After degradation of the DNA template by RNase-free DNase I, the cRNAs were purified and resuspended in diethyl pyrocarbonate-treated water. cRNA yield and integrity were examined on a 1% agarose gel.

Oocyte Preparation and Receptor Expression—Female *Xenopus laevis* (*Xenopus* I, Ann Arbor, MI) were anesthetized by 0.2% MS-222. The ovarian lobes were surgically removed from the frog and placed in calcium-free oocyte Ringer (OR2) incubation solution consisting of (in mM) 82.5 NaCl, 2.5 KCl, 1 $MgCl_2$, 1 Na_2HPO_4, and 5 HEPES; 50 units/ml penicillin, and 50 μg/ml streptomycin, pH 7.5. The frog was then allowed to recover from surgery before being returned to the incubation tank. The lobes were cut into small pieces and digested with 0.3% collagenase A (Roche Applied Science) with constant stirring at room temperature for 1.5–2 h. The dispersed oocytes were thoroughly rinsed with the above solution plus 1 mM $CaCl_2$. The stage VI oocytes were selected, and the follicular layer (if still present) was manually removed with fine forceps. The oocytes were incubated at 16 °C before injection.

Micropipettes for cRNA injection were pulled from borosilicate glass (Drummond Scientific, Broomall, PA) on a Sutter P87 horizontal puller, and the tips were cut with forceps to $\approx$40 μm in diameter. The cRNA, with proper dilution in diethyl pyrocarbonate-treated water, was drawn up into the micropipette and injected into oocytes with a Nanoject microinjection system (Drummond Scientific) at a total volume of 20–60 nl.

Electrophysiology—One to three days after cRNA injection, the oocyte was placed in a 100-μl chamber with continuous oocyte Ringer perfusion. The oocyte Ringer was used as an extracellular solution, which consisted of (in mM) 92.5 NaCl, 2.5 KCl, 1 $CaCl_2$, 1 $MgCl_2$, and 5 HEPES, pH 7.5. The chamber was grounded through an agarose bridge to prevent the influence of the cysteine modification reagent on the reference electrode. The oocytes were voltage-clamped at −70 mV to measure GABA-induced currents using a GeneClamp 500 (Axon Instruments, Foster City, CA). For the cysteine accessibility test, 1 mM MTSET was applied for 1 min. The current responses to GABA at a concentration inducing ~20% of the maximum GABA response (~EC_{20}) were examined before and after MTSET modification. For agonist/antagonist protection, a super-saturation concentration (>100-fold of EC_{50}) of agonist/antagonist was co-applied with 1 mM MTSET for 1 min to ensure adequate protection in the binding pocket.

Drug Preparation—GABA (Calbiochem) stock solution (100 mM) was prepared daily from the solid. 3-Aminopropylphosphonic acid (3-APA, Sigma) stock solution (100 mM) was prepared and frozen in aliquots before use. MTSET (Toronto Research Chemicals, Toronto, Canada) stock solution (100 mM) was prepared in pure water and frozen in aliquots. MTSET (1 mM in OR2) was freshly prepared from the stock solution for each oocyte immediately before use.

Data Analysis—The dose-response relationship of the GABA-induced current in recombinant $GABA_C$ receptors was least squares fit to the following Hill equation

$$I = \frac{I_{max}}{1 + (EC_{50}/[GABA])^n} \quad \text{(Eq. 1)}$$

where the GABA-induced current (I) is a function of the GABA concentration, EC_{50} is the GABA concentration required for inducing a half-maximal current, n is the Hill coefficient, and I_{max} is the maximum current. The maximum current was then used to normalize the dose-response curve for each individual oocyte. The average of the normalized currents for each GABA concentration was used to plot the data. All the data were presented as mean ± S.E. (standard error).

Statistics—The statistical significance of the effect of MTSET on the GABA-induced current in wild type and mutant receptors was evaluated by one-way analysis of variance with the Dunnett post test. The significance of agonist/antagonist protection of MTSET modulation was evaluated by grouped student t test using GraphPad Prism 4.0 (GraphPad Software, Inc., San Diego, CA).

Homology Modeling—Three-dimensional modeling of the ρ_1 GABA receptor amino-terminal domain was made based on the crystal structure of AChBP deposited in the Protein Data Bank (Protein Data Bank code 1I9B (11)). Low sequence homology between GABA receptor and AChBP did not allow straightforward or confident modeling by commonly used automatic methods such as Swiss-Model (21). Thus, a manual method was used. An electron density map of AChBP was calculated to 1.8 Å resolution, based on the coordinates of one of the monomers in the 1I9B Protein Data Bank entry. The AChBP model was imbedded in the electron density. With the sequence alignment as a guide, residues of the AChBP model were graphically mutated using the molecular graphics program QUANTA (Accelrys, San Diego, CA). Residues were mutated to residue types as indicated by sequence alignment along randomly chosen stretches of the AChBP sequence. The new side chain atoms were automatically best fit into the electron density by the QUANTA program. The best rotamers were chosen to fit density and avoid steric clashes with other parts of the molecule. Where deletions and insertions were made, structural regularization and the best rotamers were used to model surrounding and inserted residues. Manual movements of residues and side chains were made when the QUANTA automatic features were not able to resolve steric clashes. The parts of the sequence that were homologous provided many points between which regularization could be anchored. After the entire sequence was mutated and manually modeled, the structure was energy-minimized using the Crystallography and NMR System (CNS) program suite (22). The structural alignment program TOP (23) was used to align the modeled monomer with each of the five AChBP monomers in the 1I9B structure. Finally, the entire pentameric structure, with sequences mutated to that of the GABA receptor, was energy-minimized using CNS.

Visualization of the Binding Pocket—For three-dimensional presentation of the binding pocket, the newly identified binding residues along with the previously identified ones were mapped onto the homology model using the molecular graphics program Deep View. The resulting image was saved as a POV-Ray 3.5 scene file. The final image of the model was rendered by POV-Ray 3.6 software.

RESULTS

Location of the Scanning Regions—To determine the scanning regions, we used the AChBP-based structural model of the amino-terminal domain of ligand-gated ion channels as a reference. Fig. 1 shows the alignment of the ρ_1 GABA receptor subunit and AChBP partial sequences. We defined six potential binding loops in the GABA receptor ρ_1 subunit (Fig. 1, *underlined residues*). Since the critical residues for agonist binding in

```
                  110         120         130    cccccccc cccccc150
GABARρ1   LYLRHYWKDE RLSFPSTNNL SMTFDGRLVK KIWVPDMFFV HSKRSFIHDT
AChBP     FWQQTTWSDR TLAWNSSHSP --DQVSVPIS SLWVPDLAAY NAIS---KPE
          Loop D 61           71          79        Loop A      96

              cccccc cccccccccc c       180         190         200
GABARρ1   TTDNVMLRVQ PDGKVLYSLR VTVTAMCNMD FSRFPLDTQT CSLEIESYAY
AChBP     VLTPQLARVV SDGEVLYMPS IRQRFSCDVS G-VDTESGAT CRIKIGSWTH
                Loop E    116         126         135    Loop B

                  210       ccccc ccccccc       240         250
GABARρ1   TEDDLMLYWK KGNDSLKTDE RISLSQFLIQ EFHTTTKLAF YSSTGWYNRL
AChBP     HSREISVDPT TENSDDSEYF SQYSRFEILD VTQKKNSVTY SCCPEAYEDV
                155         Loop F      175           Loop C 195
```

FIG. 1. **Location of the cysteine scanning regions.** The partial amino acid sequence of the GABA receptor ρ_1 subunit amino-terminal domain was aligned to the sequence of the model molecule, AChBP, by ClustalW. The six loops (A–F) identified as participating in the formation of the agonist binding pocket of nicotinic receptors are *underlined*, and the key amino acid residues identified as binding site residues in nicotinic receptors and GABA receptors are in *bold*. The cysteine scanning residues of the ρ_1 GABA receptor subunit in this study are marked with a *c* in loops A, E, and F.

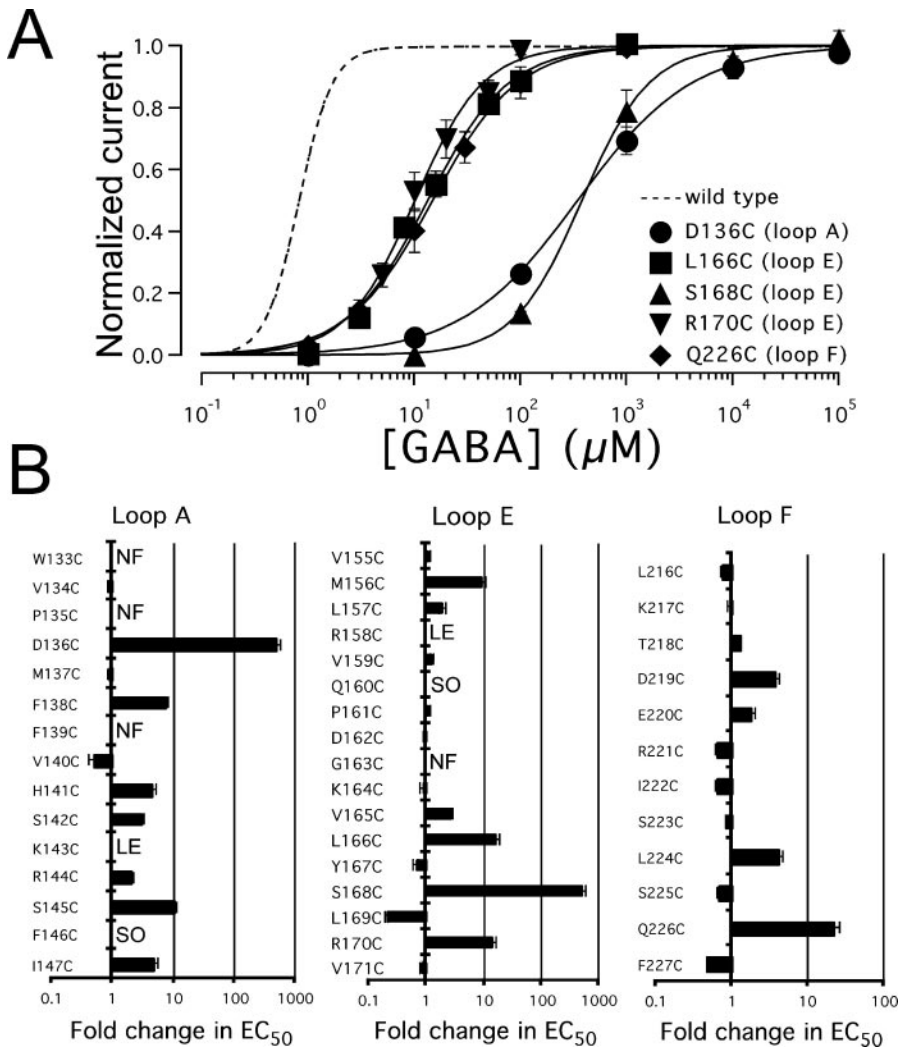

FIG. 2. **Functional properties of individual cysteine mutants of the ρ_1 GABA receptor.** *A*, dose-response curves for the mutants with a significant change in GABA sensitivity. The *lines* are least squares fits of the data to Equation 1. *B*, -fold change in EC_{50} (normalized to wild type receptor) of each cysteine mutant in the three putative binding loops. The EC_{50} values of functional mutants are listed in Table I. *NF*, nonfunctional; *LE*, low expression; *SO*, spontaneously opening.

loops B, C, and D of the ρ_1 GABA receptor subunit have been previously identified (highlighted in *bold*) (2, 13), in this study, we selected loops A, E, and F of the ρ_1 GABA receptor subunit for cysteine scanning. The *bold letters* in the AChBP highlight the amino acid residues previously identified to participate in the formation of the agonist binding pocket in nicotinic receptors. The residues of the ρ_1 GABA receptor subunit marked with a *c* above the residue are designated for cysteine scanning in this study.

Functional Properties of the Cysteine Mutants—Wild type and single cysteine mutants were individually expressed in *Xenopus* oocytes. The functional expression and dose-response relationship were examined for all the constructs. Fig. 2*A* shows dose-response relationships of representative mutants with significant changes in GABA sensitivities. Using least squares fitting to individual GABA dose-response relationships with Equation 1, we have derived EC_{50} values for the wild type and mutant receptors (Table I). -Fold changes in the EC_{50} for all mutants (normalized to the wild type receptor) are plotted in Fig. 2*B*. The alternating pattern in EC_{50} changes between L166C and V171C in loop E and between S223C and F227C in loop F may suggest a β-strand structure in these two regions.

TABLE I

EC_{50} values determined from the GABA dose-response relationship in the individual cysteine mutants of the ρ1 homomeric GABA receptor

NF, nonfunctional; LE, low expression; SO, spontaneously opening.

Loop A		Loop E		Loop F	
Mutant	EC_{50}	Mutant	EC_{50}	Mutant	EC_{50}
	μM		*μM*		*μM*
W133C	NF	V155C	0.88 ± 0.06	L216C	0.60 ± 0.03
V134C	0.66 ± 0.02	M156C	7.21 ± 0.94	K217C	0.75 ± 0.06
P135C	NF	L157C	1.53 ± 0.20	T218C	1.03 ± 0.04
D136C	387.6 ± 62.3	R158C	LE	D219C	3.02 ± 0.25
M137C	0.72 ± 0.07	V159C	0.97 ± 0.05	E220C	1.46 ± 0.11
F138C	5.94 ± 0.43	Q160C	SO	R221C	0.51 ± 0.02
F139C	NF	P161C	0.85 ± 0.05	I222C	0.50 ± 0.03
V140C	0.39 ± 0.07	D162C	0.71 ± 0.02	S223C	0.66 ± 0.01
H141C	3.65 ± 0.41	G163C	NF	L224C	3.38 ± 0.36
S142C	2.41 ± 0.17	K164C	0.69 ± 0.10	S225C	0.53 ± 0.02
K143C	LE	V165C	2.17 ± 0.12	Q226C	17.6 ± 3.58
R144C	1.66 ± 0.06	L166C	13.04 ± 1.56	F227C	0.38 ± 0.32
S145C	8.50 ± 0.51	Y167C	0.52 ± 0.05		
F146C	SO	S168C	399.9 ± 70.7		
I147C	3.92 ± 0.38	L169C	0.17±.00		
		R170C	10.84 ± 2.23		
		V171C	0.65 ± 0.06		

Note that in loop A, mutants W133C, P135C, and F139C are not functional. Interestingly, the F146C mutant exhibited a high leak current in the absence of GABA, which was blocked by picrotoxin (data not shown). This suggests that the mutation created a spontaneously opening channel. This residue is aligned to an interface residue, Lys-94, in AChBP. In loop E, G163C was nonfunctional. This residue is conserved across the subunits in the ligand-gated ion channel family and is located in the subunit interface in AChBP. In the same loop, the expression of the mutant R158C was extremely low, and the mutants L166C and S168C showed a significant increase in EC_{50}, suggesting that they may be involved in ligand binding. In fact, these three residues are aligned to the ligand binding residues Arg-104, Leu-112, and Met-114 in the AChBP (11) (Fig. 1). The mutant Q160C also showed spontaneous opening in the absence of agonist. This residue is presumably aligned to another ligand binding residue, Val-106, in AChBP. In loop F, only minor changes in channel function were observed (Table I), with the most significant change being an ~20-fold increase in the EC_{50} (Q226C).

Accessibility of the Engineered Cysteine by MTSET—To further delineate the binding pocket of the ρ_1 $GABA_C$ receptor, we examined the accessibility of the individual engineered cysteines in putative loops A, E, and F to a water-soluble thio-reactive compound, MTSET. The oocytes were treated with 1 mM MTSET for 1 min. The currents induced by a GABA concentration (~EC_{20}) before and after the MTSET treatment were recorded for each cell. The normalized current change upon treatment was calculated and plotted in Fig. 3. MTSET treatment of the wild type receptor did not significantly alter the GABA-induced current. Therefore, any significant change after MTSET treatment is due to the modification of the engineered cysteine by this compound.

For loop A, MTSET had a significant effect on the GABA-induced currents in the oocytes expressing D136C, F138C, V140C, H141C, and I147C, suggesting that residues at these positions are accessible to MTSET modification. Accessible mutants in loop E were V155C, M156C, V159C, L166C, S168C, and R170C. In loop F, most of the residues (L216C, T218C, D219C, R221C, I222C, L224C, S225C, Q226C, and F227C) were accessible. After reacting with MTSET, S225C in loop F opened in the absence of GABA.

Protection of Accessible Residues by GABA—If a cysteine residue lines the agonist binding pocket, then the binding of agonist to the receptor would block or restrict the accessibility

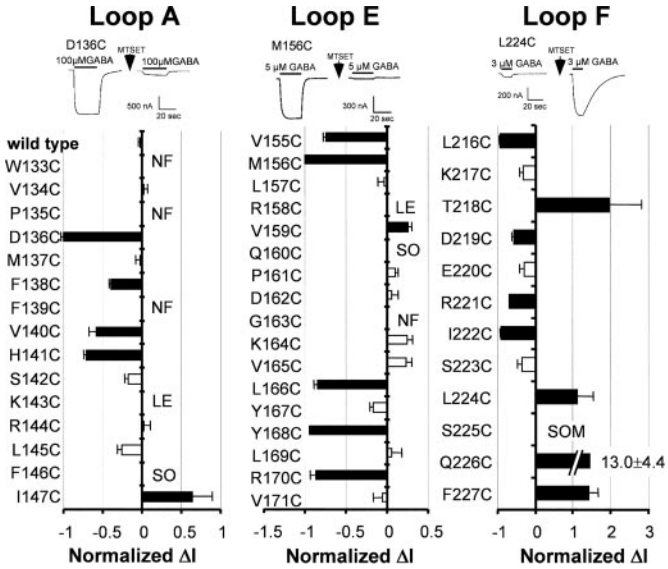

FIG. 3. **The accessibility to MTSET of the cysteine mutants in loops A, E, and F.** The wild type and individual cysteine mutants were examined for accessibility of a water soluble thio-reactive compound, MTSET (1 mM for 1 min) using a GABA concentration ~EC_{20} for each mutant as a test pulse. Examples of current traces of mutants D136C (loop A), M156C (loop E), and L224C (loop F) before and after MTSET treatment are shown above each plot. The normalized changes of the GABA-induced current after MTSET treatment ($(I_{after} - I_{before})/I_{before}$) are presented as bar graphs. A *filled bar* represents an MTSET effect on the mutant that was statistically different from the wild type control. *NF*, nonfunctional mutant; *LE*, low expression; *SO*, spontaneously opening; *SOM*, spontaneously opening after modification.

of that residue to a modification reagent. To examine whether the accessible cysteines can be blocked by GABA, a saturating concentration of GABA was co-applied with 1 mM MTSET. The co-application of GABA with MTSET significantly reduced the alteration of the GABA response by MTSET for the following mutants: D136C, F138C, and V140C in loop A and V155C, M156C, V159C, S168C, and R170C in loop E (Fig. 4). Surprisingly, none of the residues in loop F were protected by GABA from MTSET modification. These results suggest that loop F of $GABA_C$ ρ_1 receptor may not line the GABA binding pocket, whereas the GABA-protected residues in loops A and E are potential residues participating in the formation of the GABA binding pocket. However, due to global conformational changes

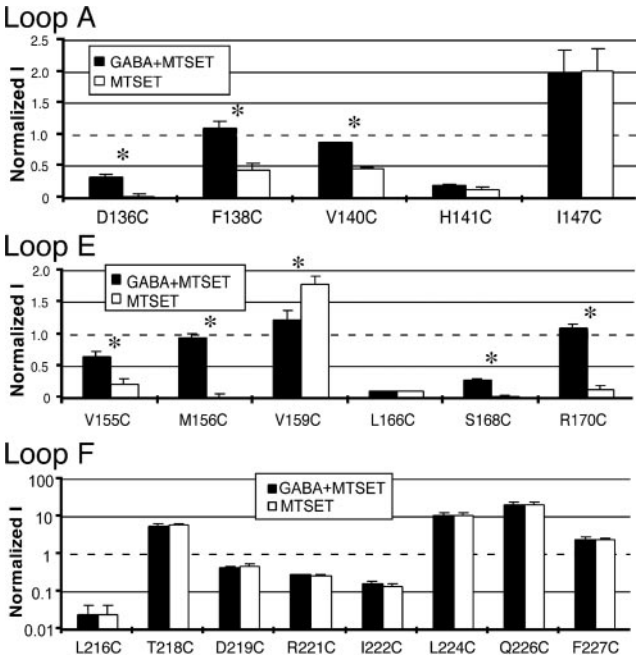

FIG. 4. **GABA protection pattern of the accessible residues in the three loops.** For all accessible residues identified, a GABA concentration ~EC_{20} was used for the test. One mM MTSET was used for modification. About 100 × EC_{50} GABA concentration was co-applied with MTSET to test protection. Note that the S225C mutant in loop F showed spontaneously opening after MTSET modification and therefore is not shown in the figure. This MTSET modification-induced opening was not protected by GABA. An *asterisk* indicates a statistically significant difference between groups in the presence and absence of GABA. The *dashed lines* indicate the control level.

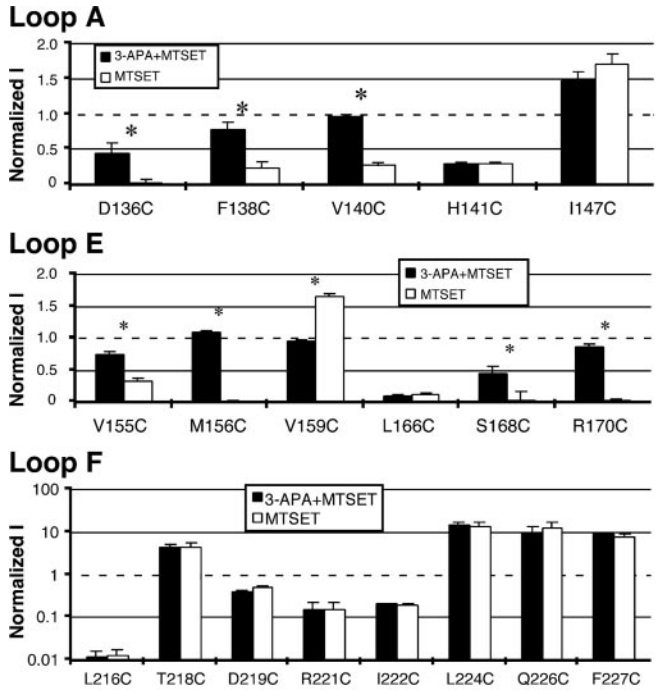

FIG. 5. **Protection pattern of the accessible residues in the three loops by competitive antagonist, 3-APA.** Each functionally accessible cysteine mutant was tested by an ~EC_{20} GABA concentration. One mM MTSET was used for modification. A saturating concentration of 3-APA was co-applied with MTSET to test for protection. An *asterisk* indicates a statistically significant difference between groups in the presence and absence of 3-APA for each mutant. The *dashed lines* indicate the control level.

induced by GABA, accessibility of residues in other regions of the receptor distant from the agonist binding pocket would potentially be altered in the presence of GABA. Therefore, a competitive antagonist protection experiment would further test whether these residues line the binding pocket.

Protection of Accessible Residues by 3-APA—3-APA is a $GABA_C$ receptor-competitive antagonist, presumably competing with the agonist for the same binding site but without inducing a similar conformational change (24). A saturating concentration of 3-APA was co-applied with 1 mM MTSET to the oocytes expressing individual cysteine mutants of the ρ_1 GABA receptor. Fig. 5 shows that 3-APA has a protection pattern similar to that for GABA. That is, the mutants D136C, F138C, and V140C in loop A and the mutants V155C, M156C, V159C, S168C, and R170C in loop E were efficiently protected by this competitive antagonist, whereas no residue in loop F was protected. These data suggest that D136C, F138C, and S142C in loop A and V155C, M156C, V159C, S168C, and R170C in loop E are most likely lining the agonist/antagonist binding pocket of the GABA ρ_1 receptor.

DISCUSSION

Identification of Novel Binding Residues in the Binding Pocket—If a residue directly interacts with the agonist, then mutation of the residue would be expected to decrease the binding affinity. With the cysteine mutations, we have identified several residues that, when mutated, reduced agonist sensitivity of the GABA receptor. The sensitivity decrease by mutation could be due to the reduction of binding affinity or a decrease in the maximum open probability (25). A pure gating effect on EC_{50}, however, is limited in the ρ_1 homomeric GABA receptor. For example, the previously established three-bind-to-open model (26) predicts that a decrease in gating efficiency of 100-fold in the ρ_1 homomeric GABA receptor would only result in an increase in the EC_{50} of ~4-fold (27). Thus, the mutations with an increase in EC_{50} for more than 4-fold, such as D136C (loop A), L166C, S168C, R170C (loop E), and Q226C (loop F), likely have a decreased binding affinity in addition to any changes in gating efficacy. The binding affinity decrease could be a direct effect of the mutation in the binding site, or the mutation could also allosterically influence binding by changing the conformation of the binding site from a distant location. These two possibilities can be further differentiated by a combination of cysteine accessibility and protection tests.

The mutants W133C, P135C, F139C (loop A), and G163C (loop E) were not functional. These mutations probably influence receptor trafficking or assembly, although we cannot rule out the possibility that the mutations directly disrupt the agonist binding site. For those mutants with minor changes in the GABA sensitivity, the role of these residues in agonist binding is probably less significant, although they might still line the binding pocket.

To further determine whether a residue lines the binding pocket, we tested the accessibility and agonist/antagonist protection of the engineered cysteines. A residue that lines the binding pocket would become less accessible when the agonist is bound. However, due to the ability of agonist to induce a global conformational change related to channel opening, it is possible that the agonist could change the conformation outside the binding pocket and make that site less accessible to the cysteine modification reagent. As a further test, we examined protection by a competitive antagonist. Although recent studies suggest that a competitive antagonist can also induce a conformational change beyond the binding site to stabilize the GABA receptor in the closed state (17, 28, 29), this antagonist-induced conformational change is distinct from that induced by the agonist (24). Thus, only when the agonist and antagonist both protect a residue from modification do we consider that residue

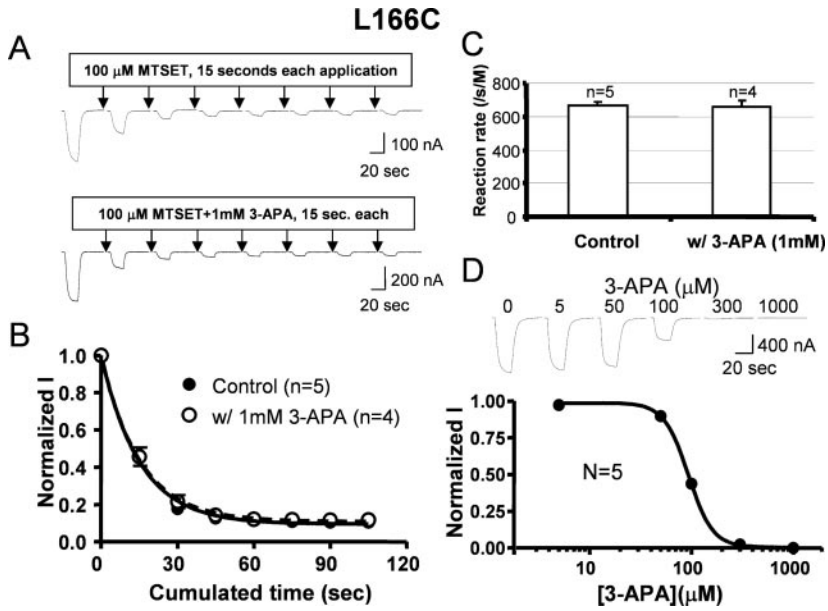

FIG. 6. **3-APA, at a saturation concentration, did not change the reaction rate of MTSET at L166C.** *A*, current traces induced by 3 μM GABA and modification by MTSET (100 μM) in the presence or absence of 3-APA (1 mM). *B*, normalized and averaged data of MTSET modification with single exponential fits (*lines*). Note that in the presence of 1 mM 3-APA, the rate of the current decay induced by MTSET modification did not change. *C*, the average MTSET reaction rate determined by fitting data from individual oocytes with a single exponential function. The rates were second-order rates (normalized to the MTSET concentration). Note that there was no significant difference in the rates in the presence or absence of 3-APA. *D*, dose-dependent inhibition of the 15 μM GABA-induced current by 3-APA, showing saturation of 3-APA inhibition at 1 mM. The *continuous line* is the least squares fit of the data to a Hill equation. The *error bars* are smaller than the *symbol*.

in the binding pocket. In this way, we have identified three novel binding residues in loop A (Asp-136, Phe-138, and Val-140) and five novel binding residues in loop E (Val-155, Met-156, Val-159, Ser-168, and Arg-170). By these criteria, no binding residues were identified in loop F, suggesting that this loop in the ρ_1 GABA receptor is not directly involved in agonist binding. Note that V140C, V155C, and V159C showed no significant change in GABA EC_{50}, suggesting that they may not directly contact the agonist but may still line the binding pocket. In contrast, the L166C and Q226C mutants were 15–20-fold less sensitive to GABA, suggesting a reduced binding affinity. The two engineered cysteine residues, however, were not protected by agonist or antagonist, indicating that they are likely outside the binding pocket. The reduction of binding affinity by these mutations could be due to an indirect/distant effect on the binding pocket.

Since our goal was to detect dramatic changes in accessibility caused by direct physical occlusion of binding residue by agonist/antagonist, we examined MTSET modification at a single time. At least in terms of detecting minor changes in accessibility, this approach is less sensitive than an examination of the reaction rate. Since L166C aligns with a binding site residue in the nicotinic receptor (11), we wanted to exclude the possibility that we were missing this potential binding site residue. We therefore examined the reaction rate of L166C to MTSET in the absence and presence of 3-APA. Fig. 6 shows that at a saturation concentration, 3-APA did not significantly change the reaction rate at L166C, further confirming our conclusion. Thus, although we cannot completely rule out the possibility that some minor binding residues might be under our detection threshold, the result gives us confidence that we did not miss crucial binding site residues.

Spontaneously Opening Channels—In this study, we found that mutations of F146C in loop A and Q160C in loop E created spontaneously opening channels. Although the S225C mutation in loop F did not create a spontaneously opening channel, modification of this engineered cysteine by MTSET made the channel open spontaneously. The mutation of Y102S in loop D (13) and several mutations in the channel lining domain (29–32) also created spontaneously opening channels. The fact that spontaneously opening channels can be created by mutations in different loops of the amino-terminal domain or in the pore-lining domain suggests that channel gating is not exclusively controlled by a single residue. Instead, the energy landscape maintaining a proper conformation of the agonist binding site and gating machinery is governed by an interconnected allosteric network. Perturbation of this allosteric network, either by agonist binding or by mutation at one of the key positions, could alter the energy landscape to stabilize the receptor in the open state. In the amino-terminal domain of the ρ_1 GABA receptor, these key positions, including residues Tyr-102 (loop D), Phe-146 (in loop A), Gln-160 (in loop E), and Ser-255 (in loop F), are distributed in multiple binding (or coupling) loops. The coordinated movement of these loops induced by agonist could be an important mechanism for channel activation. It is interesting that a mutation at a different position (L99C) in loop A of the β_2 subunit also created a spontaneously opening channel (7). In contrast, the mutant V140C in the homologous position of the ρ_1 subunit was not spontaneously active. This difference in key sites of the gating determinants may contribute to the distinct gating kinetics of $GABA_A$ and $GABA_C$ receptors.

Secondary Structure Prediction—As indicated in Fig. 2, the alternating change in EC_{50} upon cysteine mutation in the segments L166C–V171C of loop E and S223C–F227C of loop F suggests a β-strand structure. The β-strand structure of segment L166C–V171C of loop E is further supported by the alternating accessibility pattern in this region (Fig. 3). In loop F, however, the pattern of accessibility to MTSET suggests a random coil. In addition, an alternating pattern of accessibility to MTSET in the segment Asp-136–Val-140 in loop A also suggests a β-strand structure. The secondary structure predictions in these loops of the ρ_1 GABA receptor are in agreement with the crystal structure of the homologous protein, AChBP, and similar to the predictions in the homologous regions of the α_1 (8, 9) and β_2 (7) subunits of the $GABA_A$ receptor.

Comparison with the Residues Lining the GABA$_A$ Receptor Agonist Binding Pocket—$GABA_A$ and $GABA_C$ receptors share many agonists, such as GABA and muscimol, but have distinct competitive antagonists, such as bicuculline for $GABA_A$ and 1,2,5,6-tetrahydropyridine-4-yl)methylphosphinic acid for $GABA_C$. Agonist sharing suggests that they have similar overall architecture in the agonist/antagonist binding pocket, whereas the distinct antagonist profile suggests that their agonist/antagonist binding pockets are not identical. Thus, when we use agonist and competitive antagonist protection of the modification of the engineered residues as criteria for binding site residues, it would result in identification of some common and distinct residues lining the binding pocket. Fig. 7 shows all

```
GABARρ1 LYLRHYWKDE RLSFPSTNNL SMTFDGRLVK KIWVPDMFFV HSKRSFIHDT 150
GABARα1 VFFRQSWKDE RLKF-KGPMT VLRLNNLMAS KIWTPDTFFH NGKKSVAHNM 111
GABARβ2 MYFQQAWRDK RLSY-NVIPL NLTLDNRVAD QLWVPDTYFL NDKKSFVHGV 109
          Loop D                                  Loop A

GABARρ1 TTDNVMLRVQ PDGKVLYSLR VTVTAMCNMD FSRFPLDTQT CSLEIESYAY 200
GABARα1 TMPNKLLRIT EDGTLLYTMR LTVRAECPMH LEDFPMDAHA CPLKFGSYAY 161
GABARβ2 TVKNRMIRLH PDGTVLYGLR ITTTAACMMD LRRYPLDEQN CTLEIESYGY 159
                    Loop E                                Loop B

GABARρ1 TEDDLMLYWK KG-NDSLKTD ERISLSQFLI QEFHTTTKLA FYSSTGWYNR 249
GABARα1 TRAEVVYEWT REPARSVVVA EDGSRLNQYD LLGQTVDSGI VQSSTGEYVV 211
GABARβ2 TTDDIEFYWR GD--DNAVTG VTKIELPQFS IVDYKLITKK VVFSTGSYPR 207
                          Loop F                    Loop C
```

FIG. 7. **Comparison of the binding residues in GABA$_C$ and GABA$_A$ receptors.** The partial amino acid sequence of the human GABA receptor ρ_1 subunit amino-terminal domain is aligned to the homologous region of the rat α_1 and β_2 subunits. The six putative binding loops (A–F) are *underlined*. The key amino acid residues identified as binding site residues in GABA$_C$ and GABA$_A$ receptors are in *bold*.

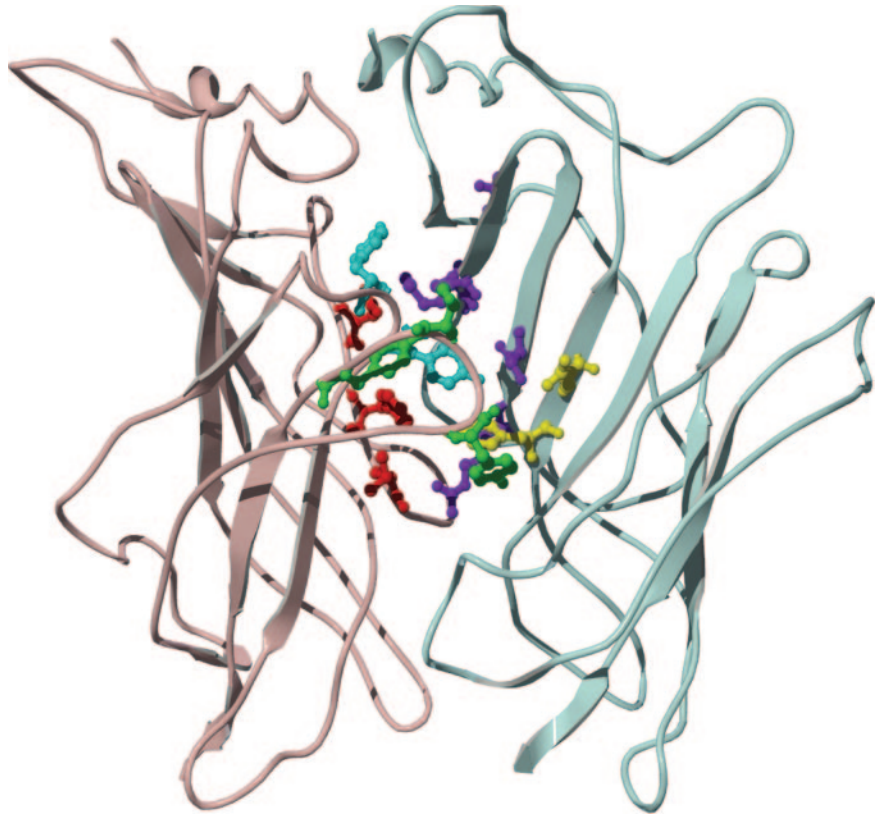

FIG. 8. **Model for the ρ_1 GABA$_C$ receptor agonist/antagonist binding pocket.** The binding residues identified in all five loops were mapped onto the homology model of the amino-terminal domain of the ρ_1 GABA receptor. These residues form a putative agonist/antagonist binding pocket in the subunit interface. (One of the five potential binding pockets in a receptor is shown.) Residues Asp-136, Phe-138, and Val-140 in loop A (*red*), Tyr-198 and Tyr-200 in loop B (*cyan*), and Tyr-241, Thr-244, and Tyr-247 in loop C (*green*) form the principal face of the binding pocket, whereas residues Tyr-102 and Arg-104 in loop D (*yellow*) and Val-155, Met-156, Val-159, Ser-168, and Arg-170 in loop E (*purple*) form the complimentary face of the binding pocket.

the binding residues identified to date in the ρ_1 (GABA$_C$) and α_1/β_2 (GABA$_A$) subunits. In loops B, C (2), and D (5, 13), the binding residues identified by site-directed mutagenesis are almost identical. In loop D, two additional binding residues, Arg-66 and Ser-68, in the α_1 subunit are recognized by the substituted cysteine accessibility method (6, 17). The corresponding residue Arg-104 in the ρ_1 subunit seems to line the binding pocket.[2] Our newly identified binding residues in loop A of the ρ_1 subunit, Phe-138 and Val-140, can find their homologous counterparts (Tyr-97 and Leu-99) in the β_2 subunit (7). However, the binding residue Aps-136 in the same loop of the ρ_1 subunit is distinct from that in the β_2 subunit. This suggests that the ρ_1 subunit in this region adopts a slightly different conformation than the corresponding region of the β_2 subunit. In loop E, our results indicate that Ser-168 and Arg-170 line the binding pocket of the ρ_1 GABA receptor, similar to the homologous residues (Thr-129 and Arg-131) in the α_1 subunit (9). In addition, we have identified three more binding residues (V155C, M156C, and V159C) in the extended region of loop E, but it belongs to a different β-strand, of the ρ_1 subunit. This region in the α_1 subunit has not yet been explored. In loop F, we could not find any residue meeting our criteria for a binding site lining residues in the ρ_1 GABA receptor. In contrast, three residues (Val-178, Val-180, and Asp-183) in loop F of the α_1 subunit have been identified as binding site residues (8). This major difference between GABA$_C$ and GABA$_A$ could, in part, underlie the functional and pharmacological diversities between these two types of GABA receptors.

Model for the ρ_1 GABA$_C$ Receptor Binding Pocket—Using cysteine scanning accessibility, we have successfully identified novel residues in the ρ_1 GABA receptor involved in GABA binding. With these data and previously identified binding residues in other loops, we were able to construct a model for the ρ_1 GABA receptor binding pocket. For a three-dimensional presentation of the agonist/antagonist binding pocket, we first built a structural model for the amino-terminal domain of the ρ_1 GABA receptor by homology modeling using AChBP as a template. The binding residues experimentally identified to date, as highlighted in Fig. 7, were then mapped onto this structural model and highlighted with the side chain (Fig. 8). The residues from loops A (*red*), B (*cyan*), and C (*green*) form one face of the binding pocket. The complementary face of the

[2] V. Torres and D. S. Weiss, personal communication.

binding pocket is formed by residues from loops D (*yellow*) and E (*purple*). Loop F is in the vicinity of the binding pocket but does not directly contribute to agonist binding. Note that all these presumed binding residues are pointing toward the putative GABA binding pocket with the exception of Val-155 and Val-159. Mutation of these residues to cysteine did not significantly alter the GABA EC_{50} of the receptor. Thus, it is possible that these residues are not in the binding pocket in the absence of agonist/antagonist, but a local conformational change induced by binding of the agonist or antagonist can alter their orientation and thus change their accessibility. Although the precise location of each residue still awaits the high resolution structure of the $GABA_C$ receptor, the excellent agreement of most experimentally identified binding residues and the homology model further strengthens our conclusion that the identified residues are actually lining the agonist binding pocket of the receptor.

REFERENCES

1. Johnston, G. (1996) *Trends Pharmacol. Sci.* **17,** 319–323
2. Amin, J., and Weiss, D. (1994) *Receptors Channels* **2,** 227–236
3. Chang, Y., Gansah, E., Chen, Y., Ye, J., and Weiss, D. (2002) *J. Neurosci.* **22,** 7982–7990
4. Amin, J., and Weiss, D. (1993) *Nature* **366,** 565–569
5. Sigel, E., Baur, R., Kellenberger, S., and Malherbe, P. (1992) *EMBO J.* **11,** 2017–2023
6. Boileau, A., Evers, A., Davis, A., and Czajkowski, C. (1999) *J. Neurosci.* **19,** 4847–4854
7. Boileau, A., Glen Newell, J., and Czajkowski, C. (2002) *J. Biol. Chem.* **277,** 2931–2937
8. Newell, J., and Czajkowski, C. (2003) *J. Biol. Chem.* **278,** 13166–13172
9. Holden, J., and Czajkowski, C. (2003) *Society for Neuroscience 33rd Annual Meeting*, *New Orleans*, *Nov. 8–12*, *2003*, *Program Number 50.10*, Society for Neuroscience, Washington, D. C.
10. Corringer, P., Le Novère, N., and Changeux, J. (2000) *Annu. Rev. Pharmacol. Toxicol.* **40,** 431–458
11. Brejc, K., van Dijk, W. J., Klaassen, R. V., Schuurmans, M., van Der Oost, J., Smit, A. B., and Sixma, T. K. (2001) *Nature* **411,** 269–276
12. Smith, G., and Olsen, R. (1994) *J. Biol. Chem.* **269,** 20380–20387
13. Torres, V., and Weiss, D. (2002) *J. Biol. Chem.* **277,** 43741–43748
14. Akabas, M., Stauffer, D., Xu, M., and Karlin, A. (1992) *Science* **258,** 307–310
15. Xu, M., and Akabas, M. (1996) *J. Gen. Physiol.* **107,** 195–205
16. Wilson, G., and Karlin, A. (1998) *Neuron* **20,** 1269–1281
17. Holden, J., and Czajkowski, C. (2002) *J. Biol. Chem.* **277,** 18785–18792
18. Sullivan, D., Chiara, D., and Cohen, J. (2002) *Mol. Pharmacol.* **61,** 463–472
19. Sullivan, D., and Cohen, J. (2000) *J. Biol. Chem.* **275,** 12651–12660
20. Chang, Y., and Weiss, D. (1999) *Nature Neuroscience* **2,** 219–225
21. Schwede, T., Kopp, J., Guex, N., and Peitsch, M. (2003) *Nucleic Acids Res.* **31,** 3381–3385
22. Brunger, A., Adams, P., Clore, G., DeLano, W., Gros, P., Grosse-Kunstleve, R., Jiang, J., Kuszewski, J., Nilges, N., Pannu, N., Read, R., Rice, L., Simonson, T., and Warren, G. (1998) *Acta Crystallogr. Sect. D Biol. Crystallogr.* **54**, 905–921
23. Lu, G. (2000) *J. Appl. Crystallogr.* **33,** 176–183
24. Chang, Y., and Weiss, D. (2002) *Nature Neuroscience* **5,** 1163–1168
25. Colquhoun, D. (1998) *Br. J. Pharmacol.* **125,** 923–948
26. Amin, J., and Weiss, D. (1996) *Proc. R. Soc. Lond. B Biol. Sci.* **263,** 273–282
27. Chang, Y., Covey, D., and Weiss, D. (2000) *Mol. Pharmacol.* **58,** 1375–1380
28. Ueno, S., Bracamontes, J., Zorumski, C., Weiss, D., and Steinbach, J. (1997) *J. Neurosci.* **17,** 625–634
29. Chang, Y., and Weiss, D. (1999) *Biophys. J.* **77,** 2542–2551
30. Chang, Y., and Weiss, D. (1998) *Mol. Pharmacol.* **53,** 511–523
31. Pan, Z., Zhang, D., Zhang, X., and Lipton, S. (1997) *Proc. Natl. Acad. Sci. U. S. A.* **94,** 6490–6495
32. Chang, Y., Wang, R., Barot, S., and Weiss, D. (1996) *J. Neurosci.* **16,** 5415–5424

Mapping the ρ_1 $GABA_C$ Receptor Agonist Binding Pocket: CONSTRUCTING A COMPLETE MODEL

Anna Sedelnikova, Craig D. Smith, Stanislav O. Zakharkin, Delores Davis, David S. Weiss and Yongchang Chang

J. Biol. Chem. 2005, 280:1535-1542.
doi: 10.1074/jbc.M409908200 originally published online November 17, 2004
